Erosion of The Supratentorial White Matter Reference for Increased Power in Longitudinal Amyloid PET

Colm J McGinnity[1], Luis Peraza[1], Richard B Joules[1], Richard G Parker[1], Robin Wolz[1], for the Alzheimer's Disease Neuroimaging Initiative
[1]IXICO, London UK

IXICO

We demonstrate that a composite reference region that includes eroded supratentorial white matter is more sensitive to changes in amyloid plaque burden than the whole cerebellum, for longitudinal [^{18}F]florbetaben PET.

BACKGROUND & AIM

The use of the supratentorial white matter (sWM) as a reference region, alone[1–7] or in composite[3], can facilitate the detection of subtle changes in amyloid plaque burden.

Investigators often erode or otherwise restrict the sWM labels to reduce the influence of signal "spill-in" from grey matter[2–4, 8], but the optimal extent of erosion is unclear, and evaluations for ^{18}F radiotracers other than [^{18}F]florbetapir are scarce[8].

Aim: Determine the optimal extent of erosion of the supratentorial white matter for use in a composite reference region, in longitudinal amyloid PET.

METHOD – STUDY DATASETS

Table 1. *Characteristics of the study datasets.*

	[^{18}F]florbetaben (FBB)	[^{18}F]florbetapir (FBP)
n (subjects)	140	557
CN/MCI/AD/SMC	94/35/11/0	231/249/19/58
Females/Males	61/79	285/272
Age at baseline (years)	71.3 ± 6.2	72.9 ± 7.4
ADNI GCA Centiloid at baseline	31.5 ± 41.5	31.0 ± 44.7
Interscan interval (years)	3.1 ± 1.0	4.8 ± 2.7

We evaluated the sensitivity of the eroded sWM using paired longitudinal amyloid PET and MR images acquired from participants who were cognitively normal (CN) or who had mild cognitive impairment (MCI), Alzheimer's disease (AD), or subjective memory complaints (SMC) at baseline (ADNI – https://adni.loni.usc.edu; Table 1).

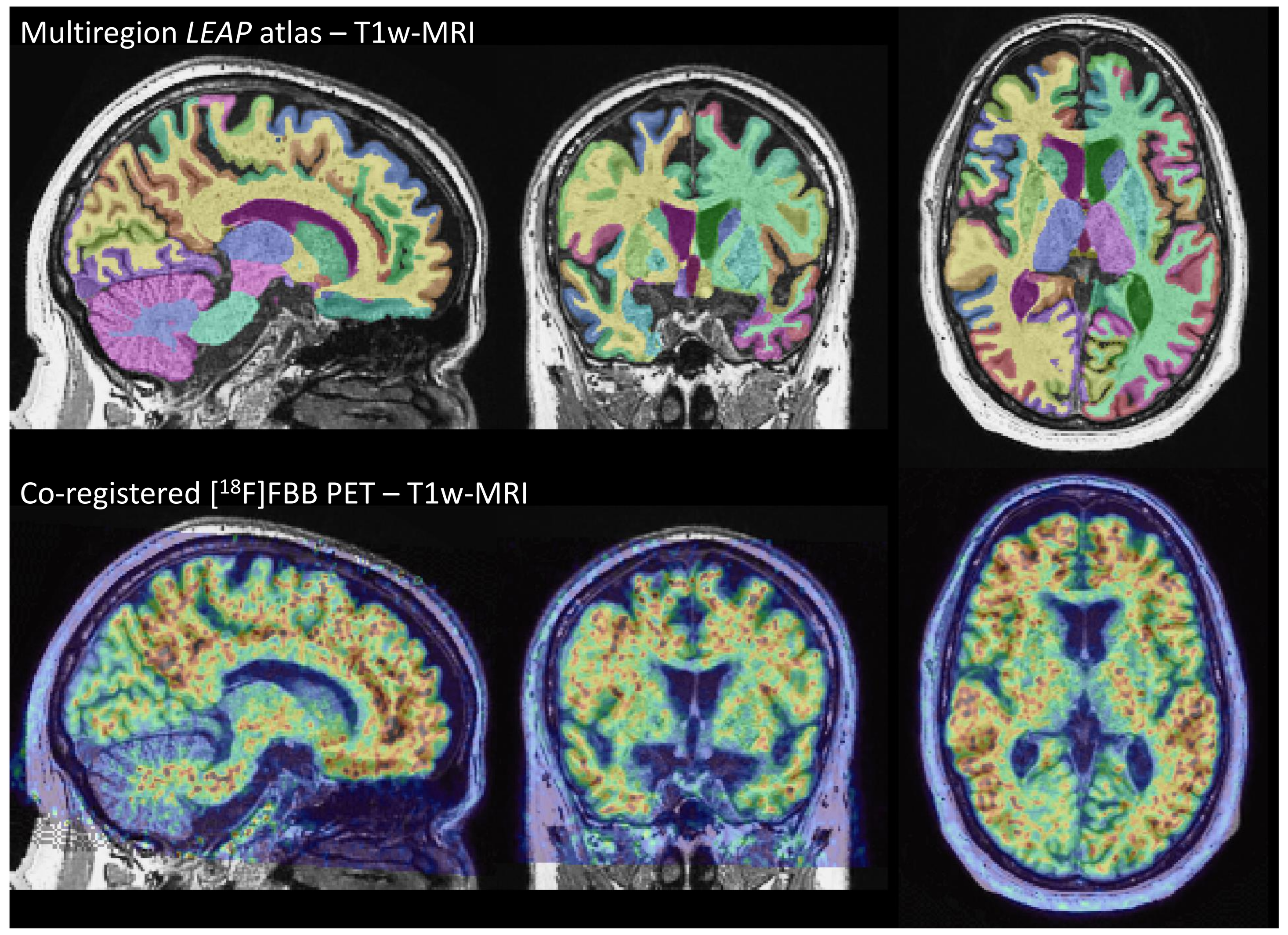

Figure 1. *Automated multi-region LEAP segmentation of the T1w-MRI (top); co-registered [^{18}F]FBB image overlaid on the T1w-MRI.*

METHOD – IMAGE PROCESSING

IXICO's multi-region *LEAP* pipeline was used to automatically segment the contemporaneous T1w-MRIs into 143 regions with high accuracy (Fig. 1). We used our in-house PET analysis pipeline to process baseline and follow-up PET scans for each participant, including frame-to-frame realignment, co-registration, erosion of the sWM, quality control, and calculation of standardized uptake value ratios (SUVRs).

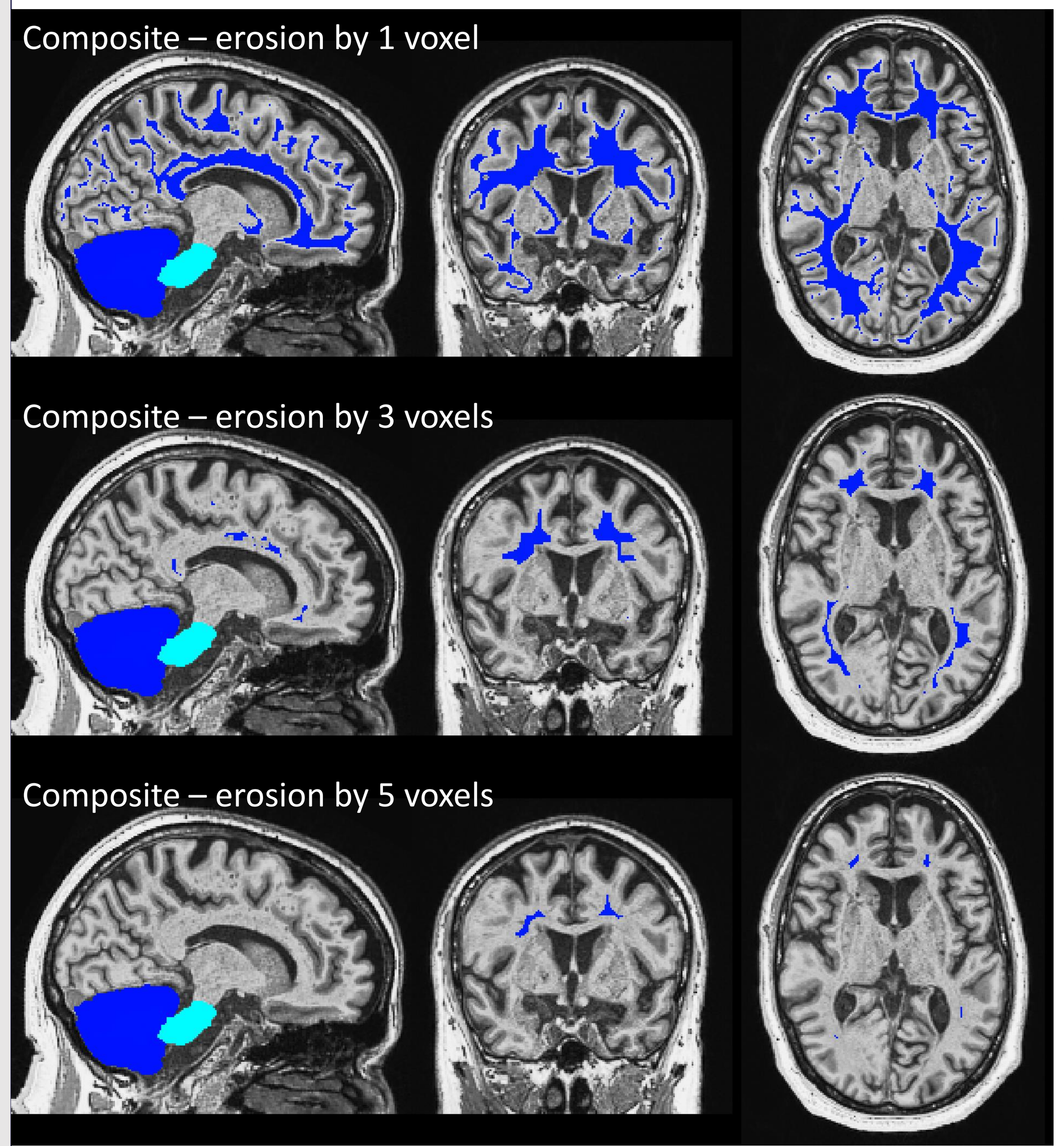

Figure 2. *The pons-sWM-WC composite reference region after erosion of the sWM by 1 (top),3 (middle), and 5 x 1 mm^3 voxels (bottom).*

The *global cortical average* (GCA) SUVR was calculated using the whole cerebellum (WC), and alternatively using a pons-sWM-WC composite whereby the sWM had been eroded by 0 – 5 x 1 mm^3 voxels (Fig. 2).

METHOD – EVALUATION

We defined two groups according to their percent change in GCA SUVR per year (%ΔSUVR/y), as calculated independently by ADNI (average for WC and composite reference regions):

- < 0.25% -> *Stable;* > 0.50% -> *Accumulator*

Our primary outcome measure was the **Hedges' g effect size** for the comparison *Accumulators* vs *Stables*. Secondary outcome measures were:

1. The area under the receiver operator characteristic curve (AUROC) and maximum balanced accuracy for prediction of group (as per [4]).
2. Correlation coefficient between baseline (BL) and follow-up (FU) GCA SUVR.
3. The percentage of participants with a non-negative ΔSUVR/y (as per [4]).
4. The correlation coefficient between ΔSUVR/y and change in Mini Mental State Examination (MMSE) score per year (as per [4]).

RESULTS

Outcome measures are reported as mean ± standard deviation over 10,000 samples (generated via bootstrapping with replacement).

For [^{18}F]FBB, the AUROCs, maximum accuracies and Hedges' gs were slightly higher with the eroded composite than with the WC (Table 2).

Table 2. *[^{18}F]FBB results – best in bold font and underlined.*

	Whole Cerebellum	Composite	Composite (erosion 1)	Composite (erosion 2)	Composite (erosion 3)	Composite (erosion 4)	Composite (erosion 5)
Volume (x 10^3 mm^3)	125 ± 13	543 ± 56	323 ± 41	230 ± 32	190 ± 26	163 ± 20	151 ± 18
Hedges' g (n=76/51)	1.765 ± 0.156	**2.101 ± 0.187**	2.081 ± 0.186	2.080 ± 0.186	2.086 ± 0.188	2.088 ± 0.190	2.075 ± 0.194
AUROC (n=76/51)	0.929 ± 0.022	**0.945 ± 0.018**	0.941 ± 0.019	0.940 ± 0.019	0.942 ± 0.019	0.943 ± 0.019	0.939 ± 0.019
Accuracy (n=76/51)	0.890 +/- 0.024	**0.894 ± 0.025**	0.892 ± 0.026	0.892 ± 0.026	0.892 ± 0.026	0.893 ± 0.026	0.891 ± 0.027
BL – FU Correlation (r)	0.9724 ± 0.0050	0.9747 ± 0.0049	0.9758 ± 0.0047	0.9765 ± 0.0046	0.9770 ± 0.0044	0.9772 ± 0.0043	**0.9774 ± 0.0042**
% Non-negative	**62.2 ± 4.1**	60.0 ± 4.1	58.5 ± 4.1	59.3 ± 4.1	59.3 ± 4.1	60.0 ± 4.1	58.5 ± 4.1
MMSE (ρ, n=140)	-0.077 ± 0.092	-0.137 ± 0.086	-0.153 ± 0.086	**-0.157 ± 0.087**	-0.155 ± 0.087	-0.147 ± 0.087	-0.140 ± 0.087

In contrast, for [^{18}F]FBP, the AUROCs and maximum accuracies were lower with the eroded composite than with the WC (Table 2).

Table 3. *[^{18}F]FBP results – best in bold font and underlined.*

	Whole Cerebellum	Composite	Composite (erosion 1)	Composite (erosion 2)	Composite (erosion 3)	Composite (erosion 4)	Composite (erosion 5)
Volume (x 10^3 mm^3)	122 ± 13	537 ± 54	318 ± 38	225 ± 29	185 ± 24	159 ± 19	147 ± 16
Hedges' g (n=317/200)	1.699 ± 0.078	**1.718 ± 0.105**	1.697 ± 0.102	1.664 ± 0.100	1.639 ± 0.099	1.613 ± 0.101	1.584 ± 0.106
AUROC (n=317/200)	**0.952 ± 0.009**	0.922 ± 0.012	0.915 ± 0.013	0.908 ± 0.013	0.905 ± 0.013	0.903 ± 0.014	0.901 ± 0.014
Accuracy (n=317/200)	**0.907 ± 0.013**	0.856 ± 0.015	0.850 ± 0.015	0.848 ± 0.015	0.847 ± 0.015	0.844 ± 0.015	0.846 ± 0.015
BL – FU Correlation (r)	0.9028 ± 0.0084	0.9220 ± 0.0204	0.9289 ± 0.0195	0.9325 ± 0.0182	0.9346 ± 0.0169	0.9357 ± 0.0158	**0.9364 ± 0.0148**
% Non-negative	65.9 ± 2.0	68.7 ± 2.0	68.9 ± 2.0	69.3 ± 2.0	70.0 ± 2.0	**70.0 ± 1.9**	69.7 ± 2.0
MMSE (ρ, n=542)	0.001 ± 0.048	-0.089 ± 0.045	-0.106 ± 0.045	-0.116 ± 0.045	**-0.118 ± 0.045**	-0.114 ± 0.045	-0.109 ± 0.045

REFERENCES

(1) Brendel M, et al. *Neuroimage* 2015; 108:450-9. doi: 10.1016/j.neuroimage.2014.11.055; **(2)** Chen K et al. *J Nucl Med* 2015; 56(4):560-6. 10.2967/jnumed.114.149732; **(3)** Landau SM et al. *J Nucl Med* 2015; 56(4): 567–574. doi: 10.2967/jnumed.114.148981; **(4)** Schwarz CG et al. *Neuroimage* 2017; 144:113-127. doi: 10.1016/j.neuroimage.2016.08.056; **(5)** Trypustsen V et al. *J Alzheimers Dis* 2015; 43(3):809-21. doi: 10.3233/JAD-131979; **(6)** Blautzik J et al. *Eur J Nucl Med Mol Imaging* 2017; 44(8):1364-1374. 10.1007/s00259-017-3666-8; **(7)** Fleisher AS et al. *Alzheimers Dement* 2017; 13(10):1117-1124. doi: 10.1016/j.jalz.2017.02.009; **(8)** Bullich S et al. *J Nucl Med* 2017; 58(8):1300-6. doi: 10.2967/jnumed.116.187351; **(9)** Lowe VJ et al. *J Nucl Med* 201; 59(10):1583-1589. doi: 10.2967/jnumed.117.204271.

CONCLUSIONS

- The **extent of erosion of the sWM had a very modest influence on the sensitivity** to longitudinal change in plaque burden, and on secondary measures.
- The sWM-containing reference regions **slightly outperformed the WC** on classification and detection tasks, **for [^{18}F]florbetaben only**.
- Further evaluation is required, using datasets with shorter interscan intervals (e.g. ≤ 2 years) and less marked between-group differences in ΔSUVR/y.
- Investigators should remain mindful of the limitations of WM-containing regions[9].